Journal of Solid State Chemistry 181 (2008) 3223–3228

Contents lists available at ScienceDirect

Journal of Solid State Chemistry

journal homepage: www.elsevier.com/locate/jssc

Structure and magnetic properties of RE_2CuIn_3 (RE = Ce, Pr, Nd, Sm and Gd)

Yuriy B. Tyvanchuk [a], Andrzej Szytuła [b], Arkadiusz Zarzycki [b], Ute Ch. Rodewald [c], Yaroslav M. Kalychak [a], Rainer Pöttgen [c,*]

[a] Faculty of Chemistry, Ivan Franko National University of Lviv, Kyryla and Mephodiya Street 6, 79005 Lviv, Ukraine
[b] Marian Smoluchowski Institute of Physics, Jagiellonian University, Reymonta 4, 30-059 Kraków, Poland
[c] Institut für Anorganische und Analytische Chemie, Universität Münster, Corrensstrasse 30, D-48149 Münster, Germany

ARTICLE INFO

Article history:
Received 16 June 2008
Received in revised form
12 August 2008
Accepted 17 August 2008
Available online 23 August 2008

Keywords:
Indium
Intermetallics
Crystal chemistry
Magnetism

ABSTRACT

The ternary copper indides $RE_2CuIn_3 \equiv RECu_{0.5}In_{1.5}$ (RE = Ce, Pr, Nd, Sm and Gd) were synthesized from the elements in sealed tantalum tubes in an induction furnace. They crystallize with the $CaIn_2$-type structure, space group $P6_3/mmc$, with a statistical occupancy of copper and indium on the tetrahedral substructure. These indides show homogeneity ranges $RECu_xIn_{2-x}$. Single crystal structure refinements were performed for five crystals: $CeCu_{0.66}In_{1.34}$ ($a = 479.90(7)$ pm, $c = 768.12(15)$ pm), $PrCu_{0.52}In_{1.48}$ ($a = 480.23(7)$ pm, $c = 759.23(15)$ pm), $NdCu_{0.53}In_{1.47}$ ($a = 477.51(7)$ pm, $c = 756.37(15)$ pm), $SmCu_{0.46}In_{1.54}$ ($a = 475.31(7)$ pm, $c = 744.77(15)$ pm), and $GdCu_{0.33}In_{1.67}$ ($a = 474.19(7)$, $c = 737.67(15)$ pm). Temperature-dependent susceptibility measurements show antiferromagnetic ordering at $T_N = 4.7$ K for Pr_2CuIn_3 and Nd_2CuIn_3 and 15 K for Sm_2CuIn_3. Fitting of the susceptibility data of the samarium compound revealed an energy gap $\Delta E = 39.7(7)$ K between the ground and the first excited levels.

1. Introduction

The rare-earth metal (RE)–transition metal (T)–indium systems have intensively been studied in the last 30 years with respect to the crystal chemical peculiarities and interesting magnetic properties [1–3]. Of the many RE–T–In systems, those with copper have most thoroughly been studied with respect to phase analyses. Several isothermal sections have been completely analysed [4].

Except scandium, ytterbium, and lutetium, the RE–Cu–In systems show extended solid solutions $RECu_xIn_{2-x}$ [5–10] with AlB_2-related structures. During the first studies at 873 K [5–8], a small AlB_2-related cell with a statistical distribution of the copper and indium atoms on the boron network was assumed based on powder diffraction data. Later on doubling of the subcell c-axis was observed, pointing to a $CaIn_2$-related structure. In general, ordering variants for such solid solutions RET_xX_{2-x} (X = element of the third, fourth, or fifth main group) with AlB_2-related structures have been observed for the compositions $RETX$ and $RET_{0.5}X_{1.5}$ (i.e. RE_2TX_3). The crystal chemical peculiarities and the group–subgroup relations starting from the aristotype AlB_2 have recently been reviewed [11]. In view of these systematic studies on the AlB_2 superstructures we have reinvestigated the $RECu_xIn_{2-x}$ systems for $x = 0.5$. Herein we report on single crystal studies and magnetic properties.

2. Experimental

2.1. Synthesis

Starting materials for the preparation of the RE_2CuIn_3 samples were ingots of the rare-earth elements (Johnson Matthey, Chempur or Kelpin), copper drops (Heraeus), and indium tear drops (Heraeus), all with stated purities better than 99.9%. In a first step the rare-earth ingots ware mechanically cut into smaller pieces and arc-melted to small buttons under an atmosphere of about 600 mbar argon in a water-cooled copper crucible [12]. The argon was purified with silica gel, molecular sieves, and titanium sponge (900 K). The pre-melting procedure strongly reduces a shattering of the elements during the strongly exothermic reaction with copper and indium.

The starting components were weighed in the atomic ratio 2:1:3 and arc-welded in small tantalum tubes under an argon pressure of about 600 mbar. The tubes were then placed in a water-cooled sample chamber [13] of a high-frequency furnace (Hüttinger Elektronik, Freiburg, Type TIG 5/300) and first heated under flowing argon with the maximum power of the generator. The exothermic reaction between the three elements was visible by the occurrence of a heat flash near ~1500 K. After 5 min the

* Corresponding author. Fax: +49 251 83 36002.
E-mail addresses: yutyv@franko.lviv.ua (Y.B. Tyvanchuk), pottgen@uni-muenster.de (R. Pöttgen).

0022-4596/$ - see front matter © 2008 Elsevier Inc. All rights reserved.
doi:10.1016/j.jssc.2008.08.020

Table 1
Crystallographic data and lattice parameters of the ternary RE_2CuIn_3 compounds (RE = Ce–Nd, Sm and Gd

Starting composition	Refined composition	Str. type	SG	a (pm)	c (pm)	Reference
$CeCu_{0.5}In_{1.5}$		AlB_2	$P6/mmm$	481.8(1)	389.9(1)	[1]
Ce_2CuIn_3		AlB_2	$P6/mmm$	482.1	385.2	[6]
2Ce:Cu:3In[a]		$CaIn_2$	$P6_3/mmc$	482.2(3)	763.3(3)	This work
	$CeCu_{0.66(2)}In_{1.34(2)}$[b]	$CaIn_2$	$P6_3/mmc$	479.90(7)	768.12(15)	This work
$CeCu_{0.8-0.4}In_{1.2-1.6}$		AlB_2	$P6/mmm$	480.4–483.5(1)	383.7–391.7(2)	[1]
$PrCu_{0.5}In_{1.5}$		AlB_2	$P6/mmm$	478.9(2)	381.2(3)	[1]
Pr_2CuIn_3		AlB_2	$P6/mmm$	480.8	386.0	[6]
2Pr:Cu:3In[a]		$CaIn_2$	$P6_3/mmc$	479.7(3)	758.5(3)	This work
	$PrCu_{0.52(2)}In_{1.48(2)}$[b]	$CaIn_2$	$P6_3/mmc$	480.23(7)	759.23(15)	This work
$PrCu_{0.5-0.2}In_{1.5-1.8}$		AlB_2	$P6/mmm$	478.2–485.3	395.8–378.9	[1]
$NdCu_{0.5}In_{1.5}$		AlB_2	$P6/mmm$	478.4(1)	380.0(2)	[1]
Nd_2CuIn_3		AlB_2	$P6/mmm$	482.1	380.9	[6]
2Nd:Cu:3In[a]		$CaIn_2$	$P6_3/mmc$	478.9(2)	752.6(2)	This work
	$NdCu_{0.53(2)}In_{1.47(2)}$[b]	$CaIn_2$	$P6_3/mmc$	477.51(7)	756.37(15)	This work
$NdCu_{0.7-0.3}In_{1.3-1.7}$		AlB_2	$P6/mmm$	477.3–481.3(1)	376.4–380.5(2)	[1]
2Sm:Cu:3In[a]		$CaIn_2$	$P6_3/mmc$	475.6(2)	743.9(2)	This work
	$SmCu_{0.46(2)}In_{1.54(2)}$[b]	$CaIn_2$	$P6_3/mmc$	475.31(7)	744.77(15)	This work
$SmCu_{0.5}In_{1.5}$		AlB_2	$P6/mmm$	470.4(1)	364.7(1)	[1]
$SmCu_{0.6-0.2}In_{1.4-1.8}$		AlB_2	$P6/mmm$	474.7–481.3(1)	372.5–369.9(1)	[1]
2Gd:Cu:3In[a]		$CaIn_2$	$P6_3/mmc$	474.4(2)	737.9(2)	This work
	$GdCu_{0.33(3)}In_{1.67(3)}$[b]	$CaIn_2$	$P6_3/mmc$	474.19(7)	737.67(15)	This work
$GdCu_{0.59-0.35}In_{1.41-1.65}$		AlB_2	$P6/mmm$	473.0–477.0(1)	369.2–367.5(1)	[1]
Gd_2CuIn_3		$CaIn_2$	$P6_3/mmc$	474.09(9)	738.57(9)	[9]

[a] Lattice parameters from Guinier powder data.
[b] Lattice parameters from diffractometer measurements.

temperature was slowly decreased in order to enhance the growth of small single crystals. At 900 K the tube was annealed for another 2 h followed by quenching, resulting in polycrystalline samples of RE_2CuIn_3. The compounds are stable in air over weeks. Single crystals exhibit metallic luster while ground powders are dark grey.

2.2. X-ray powder data

The RE_2CuIn_3 samples were characterized by Guinier powder diagrams using Cu$K\alpha_1$ radiation and α-quartz ($a = 491.30$ pm and $c = 540.46$ pm) as an internal standard. The Guinier camera was equipped with an imaging plate system (Fujifilm, BAS-1800). The hexagonal lattice parameters (Table 1) were obtained by least-squares refinements. The correct indexing was ensured by a comparison with calculated patterns [14]. The powder patterns clearly revealed the superstructure reflections for doubling of the c-axis of the AlB_2-related subcells.

2.3. Single crystal X-ray diffraction

Irregularly shaped crystals of RE_2CuIn_3 (RE = Ce, Pr, Nd, Sm, Gd) samples were directly selected from the crushed annealed samples. The crystals were glued to small quartz fibres using varnish and first checked by Laue photographs on a Buerger camera, equipped with the same Fujifilm, BAS-1800 imaging plate technique. Intensity data were collected on a Stoe IPDS II diffractometer (graphite monochromatized Mo$K\alpha$ radiation; oscillation mode) and numerical absorption corrections were applied to the data sets. All relevant crystallographic data for the data collections and evaluations are listed in Table 2.

2.4. Scanning electron microscopy

The single crystals investigated on the diffractometer and the bulk samples were analysed using a Leica 420 I scanning electron microscope with CeO_2, the rare-earth trifluorides, copper, and InAs as standards. No impurity elements heavier than sodium (detection limit of the instrument) were observed. The compositions determined semi-quantitatively by EDX were close to the ideal one.

2.5. Magnetic measurements

DC magnetic measurements of X-ray pure samples of Pr_2CuIn_3, Nd_2CuIn_3, and Sm_2CuIn_3 were carried out using a commercial MPMS SQUID magnetometer. Two types of measurements were performed: magnetic susceptibility measurements in a magnetic field of 1 kOe in the temperature range 2–300 K (from these data the effective magnetic moment μ_{eff} and the paramagnetic Curie temperature θ_p were obtained) and magnetization measurements in magnetic fields up to 50 kOe at about 2 K (in order to get the value of the pseudo-saturated magnetic moment and the character of the magnetization curve). Since the crystallites had not well-defined shapes, no demagnetization effects were taken into account.

3. Results and discussion

3.1. Structure refinements

Careful analyses of the diffractometer data sets clearly revealed the doubling of the subcell c-axis and the reflection conditions were compatible with space group $P6_3/mmc$. The atomic parameters of Tb_2CuIn_3 [10] were taken as starting values and the structures were refined with anisotropic displacement parameters for all atoms with SHELXL-97 (full-matrix least-squares on F_o^2) [15]. The 4f site was refined with mixed Cu/In occupancy for all crystals, leading to the compositions listed in Table 2. Final difference Fourier syntheses revealed no significant residual peaks. The refinements then converged to the residuals listed in Table 2 and the atomic parameters and interatomic distances listed in Tables 3 and 4 (distances exemplarily for

Table 2
Crystal data and structure refinements for RE_2CuIn_3; $CaIn_2$-type; space group $P6_3/mmc$; $Z = 2$

Empirical formula	Ce_2CuIn_3	Pr_2CuIn_3	Nd_2CuIn_3	Sm_2CuIn_3	Gd_2CuIn_3
Calculated composition	$CeCu_{0.66(2)}In_{1.34(2)}$	$PrCu_{0.52(2)}In_{1.48(2)}$	$NdCu_{0.53(2)}In_{1.47(2)}$	$SmCu_{0.46(2)}In_{1.54(2)}$	$GdCu_{0.33(3)}In_{1.67(3)}$
Lattice parameters (pm)	Table 1	Table 1	Table 1	Table 1	Table 1
Molar mass (g/mol)	335.66	344.91	346.70	356.14	369.71
Calculated density (g/cm^3)	7.28	7.55	7.71	8.12	8.55
$F(000)$	285	294	295	301	311
Absorption coefficient (mm^{-1})	28.9	30.3	31.8	34.9	38.1
Crystal size (μm^3)	$10\times20\times20$	$10\times40\times70$	$10\times30\times50$	$10\times30\times50$	$20\times30\times70$
Detector distance (mm)	60	60	60	60	60
Exposure time (min)	13.0	11.0	12.0	13.0	10.0
ω range; increment	0–180, 1.0	0–180, 1.0	0–180, 1.0	0–180, 1.0	0–180, 1.0
Integr. param. A, B, EMS	14.0, 3.5, 0.014	13.5, 3.5, 0.012	13.0, 3.0, 0.014	14.0, 3.5, 0.014	13.5, 3.5, 0.012
θ range (deg)	4–35	4–33	4–35	4–33	4–35
$h\,k\,l$ range	±7, ±7, ±12	±7, ±7, ±11	±7, ±7, ±12	±7, ±7, ±11	±7, ±7, ±11
Transm. ratio (max/min)	1.44	2.11	1.93	1.44	1.24
Total no. reflections	2169	1804	2018	1733	2021
Independent reflections	156 ($R_{int} = 0.069$)	130 ($R_{int} = 0.076$)	144 ($R_{int} = 0.080$)	125 ($R_{int} = 0.074$)	143 ($R_{int} = 0.116$)
Reflections with $I \geqslant 2\sigma(I)$	122 ($R_\sigma = 0.042$)	111 ($R_\sigma = 0.038$)	126 ($R_\sigma = 0.032$)	97 ($R_\sigma = 0.057$)	106 ($R_\sigma = 0.096$)
No. of parameters	8	8	8	8	8
GoF	1.016	0.983	1.095	0.800	0.755
$R1$ [$I > 2\sigma(I)$]	0.033	0.033	0.028	0.026	0.035
wR_2 [$I > 2\sigma(I)$]	0.067	0.058	0.062	0.039	*0.035*
$R1$ (all)	0.054	0.045	0.038	0.045	0.068
wR_2 (all)	0.070	0.060	0.063	0.040	0.038
Extinction coefficient	0.0047(18)	0.0113(19)	0.014(2)	0.0130(13)	0.0241(15)
Largest diff. peak/hole (e/Å^3)	2.31/−1.87	2.49/−1.68	2.53/−1.53	2.22/−1.06	2.77/−3.13

Table 3
Atomic positions and anisotropic displacement parameters (pm^2) of RE_2CuIn_3 (RE = Ce–Nd, Sm and Gd), space group $P6_3/mmc$

Atom	Wyckoff site	Occupancy (%)	x	y	z	$U_{11} = U_{22}$	U_{33}	U_{eq}
$CeCu_{0.66(2)}In_{1.34(2)}$								
Ce	2*b*	100	0	0	1/4	168(5)	99(5)	145(4)
Cu/In	4*f*	33(2)/67(2)	2/3	1/3	0.0338(2)	120(5)	244(7)	161(5)
$PrCu_{0.52(2)}In_{1.48(2)}$								
Pr	2*b*	100	0	0	1/4	128(5)	81(5)	112(4)
Cu/In	4*f*	26(2)/74(2)	2/3	1/3	0.0343(2)	120(5)	211(7)	150(5)
$NdCu_{0.53(2)}In_{1.47(2)}$								
Nd	2*b*	100	0	0	1/4	136(4)	83(4)	119(3)
Cu/In	4*f*	26(2)/74(2)	2/3	1/3	0.0348(2)	132(4)	208(6)	157(4)
$SmCu_{0.46(2)}In_{1.54(2)}$								
Sm	2*b*	100	0	0	1/4	105(5)	58(5)	89(4)
Cu/In	4*f*	23(3)/77(3)	2/3	1/3	0.0351(1)	110(6)	190(8)	136(5)
$GdCu_{0.33(3)}In_{1.67(3)}$								
Gd	2*b*	100	0	0	1/4	111(5)	62(6)	95(4)
Cu/In	4*f*	17(3)/83(3)	2/3	1/3	0.0349(2)	124(7)	223(12)	155(7)

The anisotropic displacement factor exponent takes the form: $-2\pi^2[(ha^*)^2U_{11}+\cdots+2hka^*b^*U_{12}]$; $U_{13} = U_{23} = 0$; $U_{12} = \frac{1}{2}{}^*U_{11}$. U_{eq} is defined as one-third of the trace of the orthogonalized U_{ij} tensor.

Table 4
Interatomic distances (pm) in the structure of $SmCu_{0.46}In_{1.54}$

Sm	6	*M*	317.7	*M*	3	*M*	279.3
	6	*M*	347.0		3	Sm	317.7
	2	Sm	372.4		1	*M*	320.2
	6	Sm	475.3		3	Sm	347.0

All distances of the first coordination spheres are listed. Standard deviations are all equal or smaller than 0.2 pm. The *M* site shows a mixed occupancy $Cu_{0.23}In_{0.77}$.

$SmCu_{0.46}In_{1.54}$). Further data on the structure refinements are available.[1]

3.2. Crystal chemistry

The AlB_2-related indium-rich intermetallic compounds RE_2CuIn_3 have been reinvestigated on the basis of single crystal X-ray diffractometer data. The earlier investigations of these compounds reported only on the AlB_2-related subcells with a statistical distribution of the copper and indium atoms on the boron network. In view of the significantly different covalent radii [16] of copper (117 pm) and indium (150 pm), one can expect a structural distortion. Indeed, in recent reinvestigations doubling of the subcell *c* parameters has been observed [9,10], pointing to a

[1] Details may be obtained from: Fachinformationszentrum Karlsruhe, D-76344 Eggenstein-Leopoldshafen, Germany, by quoting the Registry nos. CSD-419582 ($CeCu_{0.66}In_{1.34}$), CSD-419583 ($PrCu_{0.52}In_{1.48}$), CSD-419584 ($NdCu_{0.53}In_{1.47}$), CSD-419585 ($SmCu_{0.46}In_{1.54}$), and CSD-419586 ($GdCu_{0.33}In_{1.67}$).

$CaIn_2$-related atomic arrangement which allows a puckering of the honey-comb network.

The Zintl phase $CaIn_2$ shows almost full charge transfer from calcium to indium, enabling the formation of a slightly distorted tetrahedral indium network which is isoelectronic to diamond. An ionic formula splitting $Ca^{2+}[In^-]_2$ is a first approximation. With the trivalent rare-earth metals such a network structure cannot be realized since the rare-earth atoms would deliver one excess electron which cannot be accounted for In–In bonding. However, by partial substitution of the indium atoms by a monovalent coinage metal one can reduce the valence electron concentration and the formation of $CaIn_2$-related phases is possible, as it has been demonstrated for the series RE_2CuIn_3 [5–10], RE_2AgIn_3 [17–20], and $GdAu_{0.56}In_{1.44}$ [21].

Crystallographically ordered variants with the 2–1–3 composition have been observed for a variety of silicides, e.g. Er_2RhSi_3 [22,23], U_2RuSi_3 [24,25], Ce_2CoSi_3 [26], and Eu_2PdSi_3 [27–30]. Although the superstructure type Er_2RhSi_3 [22,23] allows free z parameters, the puckering of the ordered $[RhSi_3]$ networks is not pronounced. In the RE_2CuIn_3 compounds described herein, we observe a significant displacement from the subcell mirror planes, leading to stronger puckering (Fig. 1). The resulting $[Cu_xIn_{2-x}]$ networks, however, show strongly elongated tetrahedral coordination. The intralayer Cu/In–Cu/In distances in $SmCu_{0.46}In_{1.54}$ of 279 pm are much smaller than the interlayer Cu/In–Cu/In distance of 320 pm. Thus we observe much stronger bonding interactions within the layers. The intralayer distance is slightly longer than the sum of the covalent radii of 267 pm for Cu+In [16].

Although several of the investigated crystals had compositions close to RE_2CuIn_3, no further superstructure reflections which indicate an ordering of copper and indium have been observed. Nevertheless, we expect a large degree of short-range order in the samples. All crystals showed enlarged U_{33} displacement parameters (Table 3) for the mixed occupied 4*f* sites. This is a consequence of the Cu/In disorder. In view of the missing superstructure reflections (an ordered model needs an enlargement of the cell in *a*/*b* direction; for details see [11]), one can only speculate about an ordered model. As is evident from the compositions refined for the present single crystals as well as from the initial X-ray powder investigations [1], these copper compounds have homogeneity ranges $RECu_xIn_{2-x}$. Thus, a small deviation from $x = 0.5$ prevents long-range ordering. All the samples most likely contain $RECu_{0.5}In_{1.5}$ as the main phase besides small amount with slightly larger and smaller x values.

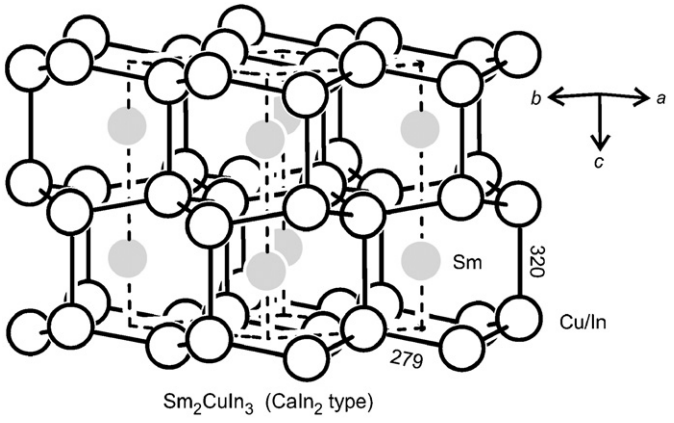

Fig. 1. View of the Sm_2CuIn_3 structure approximately along the [110] direction. The three-dimensional $[CuIn_3]$ network and relevant interatomic distances are indicated.

3.3. Magnetic behaviour

Preliminary susceptibility measurements on Pr_2CuIn_3 and Nd_2CuIn_3 samples have been performed some time ago by Siouris et al. [6]. These authors reported paramagnetic behaviour with $\mu_{eff} = 3.48\,\mu_B$ and $\theta_P = -3$ K for Pr_2CuIn_3 and $\mu_{eff} = 3.75\,\mu_B$ and $\theta_P = -12$ K for Nd_2CuIn_3. While no magnetic ordering has been observed down to 4.2 K for Pr_2CuIn_3, antiferromagnetic ordering at 12 K was observed for the Nd_2CuIn_3 sample. Since the lattice parameters of the samples differed from our values (most likely due to a different composition $PrCu_xIn_{2-x}$ and $NdCu_xIn_{2-x}$), we have reinvestigated the magnetic behaviour. Susceptibility data for Sm_2CuIn_3 are reported herein for the first time.

The investigated RE_2CuIn_3 compounds (RE = Pr, Nd, Sm) are antiferromagnets at low temperatures. The temperature dependencies of the magnetic susceptibility give the characteristic maxima for the transitions from an antiferromagnetic to a paramagnetic state at 4.7 K for RE = Pr and Nd and 15 K for RE = Sm (see Fig. 2).

The magnetization curves at 2 K are non-linear functions of the external magnetic field up to 50 kOe for RE = Pr and Nd but linear in the case of RE = Sm. The values of the magnetic moment at 2 K and 50 kOe are equal to 1.01 μ_B (RE = Pr), 1.03 μ_B (RE = Nd) and 0.02 μ_B (RE = Sm). All these values are smaller than the values for the free RE^{3+} ions equal to 3.2 μ_B (Pr), 3.27 μ_B (Nd) and 0.71 μ_B

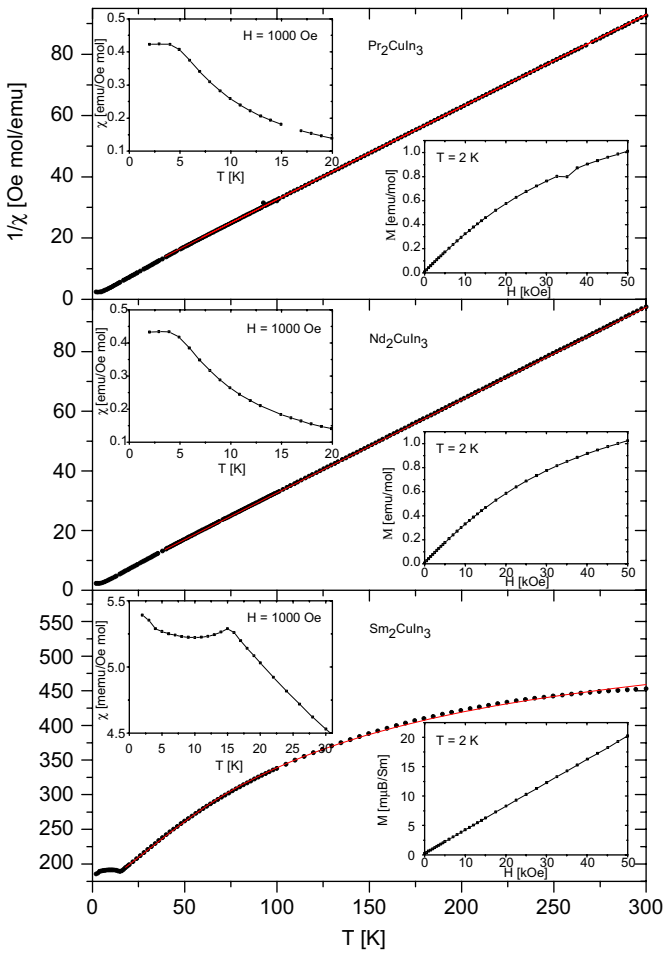

Fig. 2. Temperature dependence of the reciprocal magnetic susceptibility of some RE_2CuIn_3 (RE = Pr, Nd, Sm) compounds. The solid lines represent the fits to the experimental data. The upper insets show the low-temperature magnetic susceptibility in vicinity of the magnetic phase transitions. The bottom insets display the magnetization isotherms measured at 2 K.

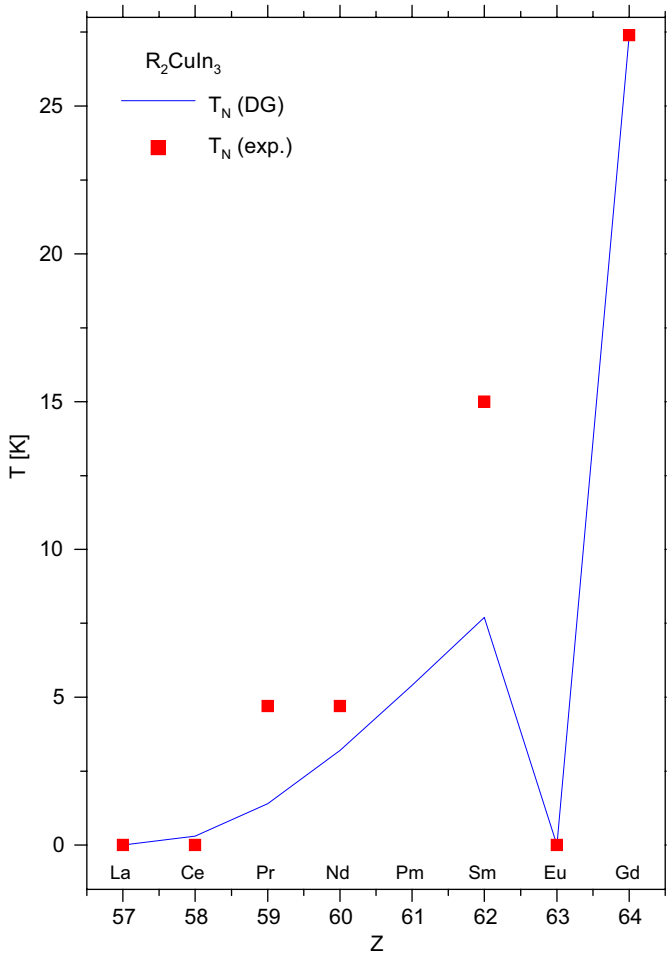

Fig. 3. Comparison of the Néel temperatures for the RE_2CuIn_3 (RE = Pr, Nd, Sm) compounds, observed (symbols) and calculated (line) from the de Gennes relation. The calculated values are normalized to the Néel temperature of Gd_2CuIn_3 from Ref. [9].

(Sm). Above the Néel temperature the reciprocal magnetic susceptibility obeys the Curie–Weiss law with the paramagnetic Curie temperatures equal to −5.3(1) K for RE = Pr and −4.70(5) K for RE = Nd and the effective magnetic moment equal to 3.56 μ_B for RE = Pr and 3.55 μ_B for RE = Nd. These values are near those for the free RE^{3+} ions: 3.58 and 3.62 μ_B, respectively.

A different dependence is observed for Sm_2CuIn_3, as is typical for the Sm-intermetallic compounds in which the first excited state of the Hund's rule multiplet ($J=\frac{7}{2}$) is very close to the ground state ($J=\frac{5}{2}$).

The temperature dependence of the magnetic susceptibility is described by the formula:

$$\chi = \frac{g_J^2 \mu_B^2 N}{3kT} \frac{m_1^2 + m_2^2 e^{-\Delta E/kT}}{1 + e^{-(-\Delta E/kT)}}$$

where N is the Avogadro number, k is Boltzmann's constant, m_1 and m_2 are the effective quantum numbers of the ground and the first excited levels, and ΔE is the energy gap between them, g_J is the Landé splitting factor, and μ_B is the Bohr magneton. χ_0 is a temperature independent part of the magnetic susceptibility including the diamagnetic core correction, the Pauli susceptibility of the electron gas and the Van Vleck temperature independent paramagnetism. Fitting the experimental data to the above relation gives the following values $m_1 = 0.76(1)$, $m_2 = 1.18(1)$, $\Delta E = 39.7(7)$ K and $\chi_0 = 1.72(1) \times 10^{-3}$ emu/mol. The value 0.76(1) is near to the data for the free Sm^{3+} ion equal to 0.85. The value of the energy gap is near to the one observed in SmNiAl (50 K) [31].

The phases presented here are antiferromagnetic at low temperatures and their Néel points increase along the series from 4.7 K for RE = Pr and Nd to 15 K for RE = Sm. In these compounds the RE–RE interatomic distances are large; about 470 pm in the (001) plane and about 360 pm between the planes. The magnetic ordering in the series is stabilized by the RKKY interactions. In this interaction the Néel temperatures are proportional to the de Gennes factor $DG = (g_J-1)^2 J(J+1)$. A comparison of the experimental results with the DG relation is presented in Fig. 3. The observed disagreement is most like caused by the interactions [32].

4. Conclusions

The RE_2CuIn_3 indides with RE = Ce, Pr, Nd, Sm and Gd have been studied by single crystal X-ray diffraction. They crystallize with a $CaIn_2$-type structure, space group $P6_3/mmc$ with a statistical occupancy of the indium site by copper and indium. Susceptibility measurements reveal antiferromagnetic ordering at $T_N = 4.7$ K for Pr_2CuIn_3 and Nd_2CuIn_3 and 15 K for Sm_2CuIn_3.

Acknowledgments

We thank Dr. F.M. Schappacher for the work at the scanning electron microscope. This work was financially supported by the Deutsche Forschungsgemeinschaft. Yu.B.T. is indebted to the DAAD for a research stipend.

References

[1] Ya.M. Kalychak, V.I. Zaremba, R. Pöttgen, M. Lukachuk, R.-D. Hoffmann, Rare earth–transition metal–indices, in: K.A. Gschneider Jr., V.K. Pecharsky, J.-C. Bünzli (Eds.), Handbook on the Physics and Chemistry of Rare Earths, vol. 34, Elsevier, Amsterdam, 2005, pp. 1–133 (Chapter 218).
[2] A. Szytuła, J. Leciejewicz, Handbook of Crystal Structures and Magnetic Properties of Rare Earth Intermetallics, CRC Press, Boca Raton, 1994.
[3] A. Szytuła, Magnetic properties of ternary intermetallic rare-earth compounds, in: K.H.J. Buschow (Ed.), Handbook of Magnetic Materials, vol. 6, Elsevier, Amsterdam, 1991, pp. 85–180 chapter 2.
[4] Ya.M. Kalychak, Izv. RAN Metally 4 (1998) 110.
[5] V.M. Baranyak, O.V. Dmytrakh, Ya.M. Kalychak, P.Yu. Zavalij, Izv. Akad. Nauk USSR Inorg. Mater. 24 (1988) 873.
[6] I.M. Siouris, I.P. Semitelou, J.K. Yakinthos, J. Alloys Compd. 297 (2000) 26.
[7] I.M. Siouris, I.P. Semitelou, J.K. Yakinthos, R.R. Arons, W. Schäfer, J. Magn. Magn. Mater. 226–230 (2001) 1128.
[8] I.M. Siouris, I.P. Semitelou, J.K. Yakinthos, W. Schäfer, R.R. Arons, J. Alloys Compd. 314 (2001) 1.
[9] A. Szytuła, Yu. Tyvanchuk, T. Jaworska-Gołąb, A. Zarzycki, Ya. Kalychak, Ł. Gondek, N. Stüsser, Chem. Met. Alloys 1 (2008) 97.
[10] A. Szytuła, A. Arulraj, S. Baran, D. Kaczorowski, B. Penc, N. Stüsser, Solid State Commun. 147 (2008) 61.
[11] R.-D. Hoffmann, R. Pöttgen, Z. Kristallogr. 216 (2001) 127.
[12] R. Pöttgen, Th. Gulden, A. Simon, GIT Labor Fachzeitsch. 43 (1999) 133.
[13] D. Kußmann, R.-D. Hoffmann, R. Pöttgen, Z. Anorg. Allg. Chem. 624 (1998) 1727.
[14] K. Yvon, W. Jeitschko, E. Parthé, J. Appl. Crystallogr. 10 (1977) 73.
[15] G.M. Sheldrick, SHELXL-97, Program for Crystal Structure Refinement, University of Göttingen, Germany, 1997.
[16] J. Emsley, The Elements, Oxford University Press, Oxford, 1999.
[17] L.V. Sysa, Y.M. Kalychak, Izv. RAN Metally 3 (1997) 126.
[18] J.P. Semitelou, J. Siouris, J.K. Yakinthos, W. Schäfer, D. Schmitt, J. Alloys Compd. 283 (1999) 12.
[19] J. Siouris, J.P. Semitelou, J.K. Yakinthos, W. Schäfer, Physica B 276–278 (2000) 582.
[20] I.M. Siouris, I.P. Semitelou, J.K. Yakinthos, J. Magn. Magn. Mater. 281 (2004) 394.
[21] R. Pöttgen, G. Kotzyba, E.A. Görlich, K. Latka, R. Dronskowski, J. Solid State Chem. 141 (1998) 352.
[22] B. Chevalier, P. Lejay, J. Etourneau, P. Hagenmuller, Solid State Commun. 49 (1984) 753.

[23] R.E. Gladyshevskii, K. Cenzual, E. Parthé, J. Alloys Compd. 189 (1992) 221.
[24] R. Pöttgen, P. Gravereau, B. Darriet, B. Chevalier, E. Hickey, J. Etourneau, J. Mater. Chem. 4 (1994) 462.
[25] B. Chevalier, R. Pöttgen, B. Darriet, P. Gravereau, J. Etourneau, J. Alloys Compd. 233 (1996) 150.
[26] R.A. Gordon, C.J. Warren, M.G. Alexander, F.J. DiSalvo, R. Pöttgen, J. Alloys Compd. 248 (1997) 24.
[27] R. Mallik, E.V. Sampathkumaran, M. Strecker, G. Wortmann, P.L. Paulose, J. Magn. Magn. Mater. 185 (1998) L135.
[28] S. Majumdar, R. Mallik, P.L. Paulose, E.V. Sampathkumaran, Physica B 259–261 (1999) 166.
[29] S. Majumdar, R. Mallik, E.V. Sampathkumaran, P.L. Paulose, K.V. Gopalakrishnan, Phys. Rev. B 59 (1999) 4244.
[30] U.Ch. Rodewald, R.-D. Hoffmann, R. Pöttgen, E.V. Sampathkumaran, Z. Naturforsch. 58b (2003) 971.
[31] N.C. Tuan, V. Sechovsky, M. Diviš, P. Svoboda, H. Nakotte, F.R. de Boer, N.H. Kim-Ngan, J. Appl. Phys. 73 (1993) 5677.
[32] D.R. Noakes, G.H. Shenoy, Phys. Lett. 91A (1982) 35.